Draft version October 3, 2018
Typeset using LaTeX **preprint2** style in AASTeX62

Quenching From the Outside-In: Finding MISFIReD Analogues in Illustris

Claire Kopenhafer, Stephanie Tonnesen, and Tjitske K. Starkenburg

ABSTRACT

The standard view of galaxy evolution posits that stars form from the inside-out, from center to edge. This leaves galaxy centers dominated by red light from old stars, while new stars are forming primarily at the outskirts. An observational sample known as the Measured Inner Star Formation In Red Disk Galaxies (MISFIReD; Tuttle & Tonnesen in prep.) sample contains galaxies that instead have red disks and recent star formation in their centers. We searched the Illustris cosmological simulation (Vogelsberger et al. 2014a) for a population of galaxies analogous to the MISFIReD sample using a series of photometric and spectral selection criteria. Our search yielded 70 analogue galaxies that meet the criteria of having red outskirts ($g - r > 0.655$ within 2 kpc $< r < 2R_{0.5M}$) and star formation within the last 1 Gyr in the central 2 kpc (D4000 < 1.4). We found that 61 of these galaxies not only have recent central star formation, but their central 2 kpc are actually younger than their edges ($1R_{0.5M} < r < 2R_{0.5M}$). Our analogues have centrally-concentrated star formation and gas mass, but low overall star formation rate and gas mass compared to their parent sample. These trends, along with the presence of older stars at the outskirts, suggest these analogue galaxies and, by extension, the MISFIReD galaxies, may be quenching their star formation from the outside-in, contrary to the typical view of galaxy evolution.

1. INTRODUCTION

The typical picture for disk galaxy evolution has the stars in the center forming before those at the outskirts. Moreover, disk galaxies are expected to quench first at their center. The center then becomes dominated by older stars, causing it to look redder compared to the disk and its many younger, bluer stars. This model of galaxy evolution can be described as "inside-out". Recently, however, a population of galaxies was found that appear to be the inverse of this picture (Tuttle & Tonnesen in prep.). Known as Measured Inner Star Formation In Red Disk Galaxies, or MISFIReD, these galaxies have red disks instead of blue, and show evidence of central star formation within the last 1 Gyr. These galaxies largely belong to the green valley, a region of the optical color-magnitude diagram typically associated with galaxies that are transitioning between the "blue" star-forming to "red" quiescent phases of galaxy evolution. It is assumed that galaxies transition by quenching, moving from blue to red (Faber et al. 2007), though it is also possible for galaxies to revive their star formation and move from red to blue (Salim et al. 2012).

As a complement to observations, simulations—especially cosmological simulations—can help disentangle the physical processes going on behind the observations. To gain insight into the MISFIReD sample, this work searches for an analogous sample in the Illustris cosmological

Corresponding author: Claire Kopenhafer EMAIL

simulation (Vogelsberger et al. 2014a,b; Genel et al. 2014). Illustris has a wide variety of data available from post-processing, including the work of Nelson et al. (2015), mock broadband images (Torrey et al. 2015), and merger histories (Rodriguez-Gomez et al. 2015). While simulations cannot recreate our actual universe with perfect accuracy or completeness, we can account for this by comparing our analogues to a parent population within the simulation, rather than directly to observations. This way, we can determine what makes any analogue galaxies unique within the simulation, in order to guide future observations of galaxies like the MISFIReD sample.

This paper is organized as follows: Section 2 details the photometric and spectral selection criteria used to find the MISFIReD analogue galaxies within Illustris. Section 3 describes the properties of the analogues that were discovered, covering the stellar populations (Sections 3.1 and 3.2), the gas (Sections 3.3 and 3.4), and interactions with surrounding galaxies (Sections 3.5 and 3.6). These results are used to answer three questions posed in Section 4 that interrogate the efficacy of the selections (Section 4.1), what is going on with the analogue sample (Section 4.2), and what could be causing these trends (Section 4.3). Finally, Section 5 presents the overall conclusions from this work.

2. METHODS

Our MISFIReD analogues were selected from the $z = 0$ snapshot of Illustris using a series of photometric and spectral selection criteria. The photometric criteria relied on the mock stellar observations of Torrey et al. (2015). Mock spectra were generated using the Flexible Stellar Population Synthesis (FSPS) code (Conroy et al. 2009; Conroy & Gunn 2010; Foreman-Mackey et al. 2014), as described in Section 2.3. Information about galaxy properties, such as their total stellar mass and stellar half mass radius, was taken from the Illustris data release (Nelson et al. 2015). A summary of the selection criteria can be found in Table 1.

Criterion	Number
$M_* > 10^{10}$ M$_\odot$	6947
$M_r < -19$	6865
$M_* < 10^{12}$ M$_\odot$ and $R_{0.5M} > 2$ kpc	**6839**
$g - r > 0.655$ for $r > 2$ kpc	1504
D4000 < 1.4 for $r < 2$ kpc	70

Table 1. Number of galaxies from each sequential selection, both photometric and spectral. The sample in bold is referred to as the *parent* sample throughout this text. The others are named for the quantity on which the selection was made (e.g., *g-r* and *D4000*).

2.1. *Photometric Criteria*

Our photometric selections were made using the mock broadband observations from Torrey et al. (2015), analyzed with `astropy` (Astropy Collaboration et al. 2018) and `photutils` (Bradley et al. 2018). At $z = 0$ in Illustris, broadband mocks are only available for galaxies with total stellar mass $M_* > 10^{10}$ M$_\odot$, which is 6947 galaxies. Each galaxy was imaged from four different viewing angles. Under the assumption that galaxies should be brightest when approximately face on, we restricted our selection to the view that was brightest in the SDSS r-band. Our first selection required r-band absolute magnitude $M_r < -19$, yielding 6865 galaxies.

We then removed galaxies with $M_* > 10^{12}$ M$_\odot$, as we could safely assume these galaxies were ellipticals. We also required the galaxies to have $R_{0.5M} < 2$ kpc, where $R_{0.5M}$ is the stellar half mass radius. This latter requirement removed galaxies which would not fit our radial binning procedure; see Section 3.1. These 6839 galaxies comprise our *parent* sample.

Our final selection was for red outskirts with little-to-no star formation using a color cut of

$g-r > 0.655$ in the 2 kpc $< r < 2R_{0.5M}$ region. The inner radius of 2 kpc was chosen to exceed the minimum spatial resolution of Illustris as well as to approximate the actual size of the SDSS spectral fiber at $z = 0.05$, which is the highest redshift in the MISFIReD observational sample. We found that 1504 galaxies met this criterion, forming our *g-r* sample.

2.2. *Star Formation Rate and History*

We calculated star formation histories from the star particle formation times, using bins of 10 Myr. We made the additional assumption that the star formation rate within the last 10 Myr equals the current instantaneous star formation rate of the gas. Including the instantaneous SFR helps compensate for the lack of star formation rate information in the last $\sim$ 200 Myr. This lack of information is inherent to Illustris, as the SFR throughout the galaxy is too low to accumulate the 10^6 $M_\odot$ required for an Illustris particle to be created. The star formation histories are necessary to model the stellar spectra of the galaxies, as discussed in the next section.

Later in this paper we will reference various specific star formation rates for Illustris galaxies, as well as star formation efficiencies. To calculate the specific star formation rate (sSFR) of a region, the desired SFR—either instantaneous or averaged over a period of time—is divided by the mass of stars within that same region. Star formation efficiencies (SFEs) are calculated in a similar manner, but using the mass of gas elligible to form stars instead of the mass of existing stars. In Illustris, gas is elligible to form stars if it has a density $\rho > 0.13$ cm^{-3} (Vogelsberger et al. 2014b; Springel & Hernquist 2003). Both sSFR and SFE have units of yr^{-1}.

2.3. *Mock Spectra and D4000*

We used the Flexible Stellar Population Synthesis (FSPS) code of Conroy et al. (2009) (updated in Conroy & Gunn 2010), with the Python interface from Foreman-Mackey et al. (2014), to generate mock spectra for the inner $r < 2$ kpc region of our *parent* sample. Our spectra were calculated using the MIST isochrones (Choi et al. 2016; Dotter 2016; Paxton et al. 2011, 2013, 2015) and the Miles spectral library (Sánchez-Blázquez et al. 2006; Falcón-Barroso et al. 2011). We used a Chabrier (2003) IMF. To remain consistent with the mock observations used for the photometric selections, we employed the same Charlot & Fall (2000) dust model used in Torrey et al. (2015). This model uses an effective absorption of $\tau = 1.0(\lambda/0.55\ \mu\text{m})^{-0.7}$, which is reduced by a factor of 3 for stars older than 3×10^7 yr.

To calculate the D4000 measure, we used the popular narrow definition from Balogh et al. (1999). This takes the ratio of the 4000–4100 Å band to the 3850–3950 Å band. Galaxies from the *g-r* sample with D4000 < 1.4 in the inner 2 kpc comprise our final selection, the *D4000* sample.

3. RESULTS

Here we lay out some of the properties of the *D4000* sample, especially with respect to the *g-r* and *parent* samples (see Section 2.1). The first 4 subsections relate to the formation of stars—past, present, and future—within these galaxies. The last two look at two possible explanations for why the *D4000* galaxies might differ from the *parent* sample.

3.1. *Stellar Mass Growth*

To understand how our sample of *D4000* galaxies grew over time, we first placed star particles into radial bins based on their positions r at $z = 0$ relative to the most bound particle in the galaxy. These bins were $r < 2$ kpc, 2 kpc $< r < 1R_{0.5M}$, $1R_{0.5M} < r < 2R_{0.5M}$, and $r > 2R_{0.5M}$, where $R_{0.5M}$ is the stellar half mass radius. We then used the particle formation times and initial mass to track the growth history of stellar mass in each radial bin. To

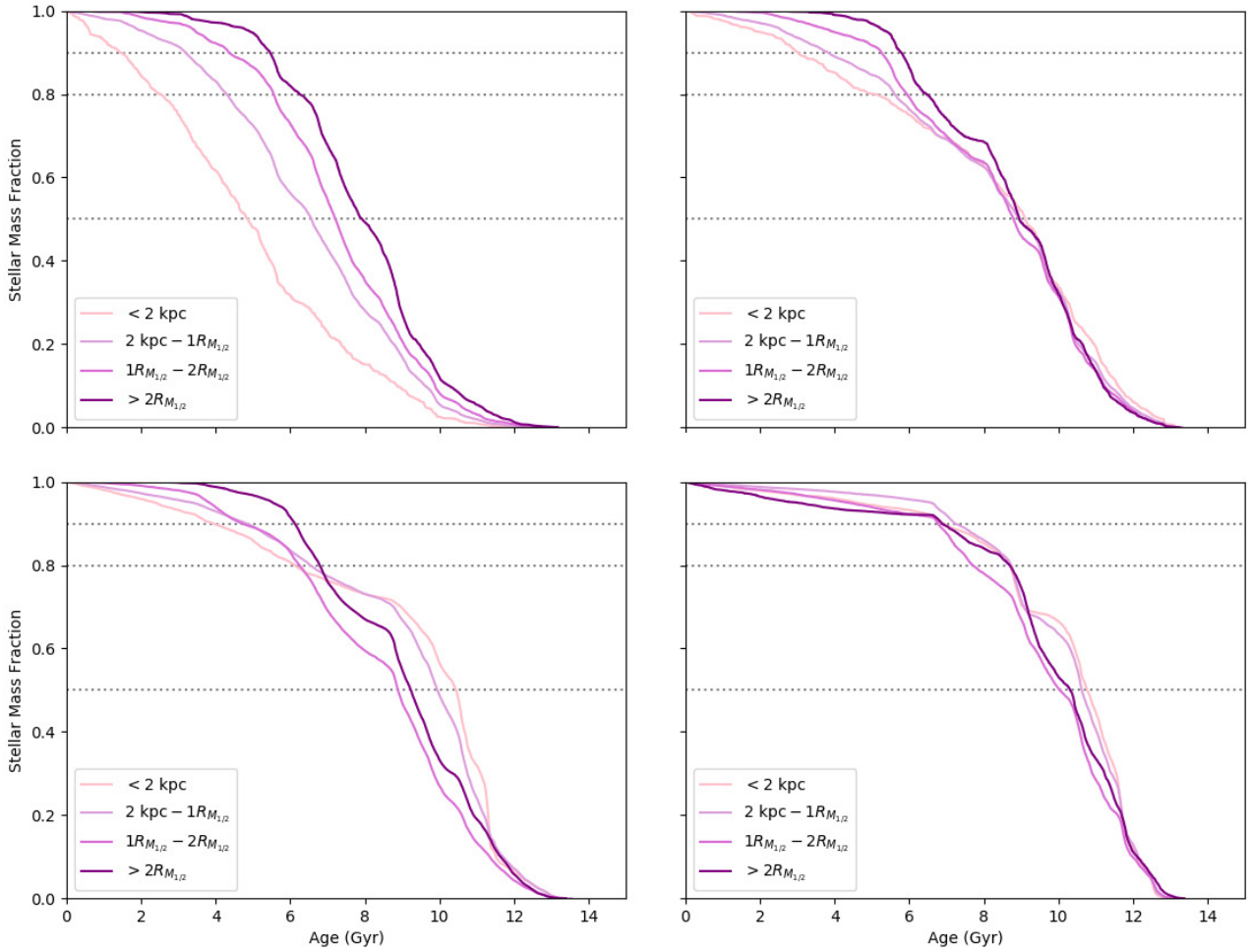

Figure 1. Relative stellar mass growth in different radial bins ($r < 2$ kpc, 2 kpc $< r < 1R_{0.5M}$, $1R_{0.5M} < r < 2R_{0.5M}$, and $r > 2R_{0.5M}$). Each bin is normalized to its final M_*. Dashed lines indicate the 50%, 80%, and 90% mass fractions. The lower right image shows a galaxy that does *not* show age-inversion at the level of 80% mass growth; see Section 3.1.

facilitate comparison, this growth is expressed as a fraction of the sum of initial star particle masses. This sum is larger than the current stellar mass, as star particles lose mass over time. A similar analysis was performed on the CALIFA observational sample by Pérez et al. (2013) assuming minimal radial stellar migration over the galaxy lifetimes. Rather than track the positions of each Illustris star particle and host galaxy back through time, we make this same assumption with our own analysis to more closely align with observational restrictions.

Four examples of this stellar mass growth history are seen in Figure 1. All four of these galaxies come from our *D4000* sample. The dashed lines show where the bins have formed 50%, 80%, and 90% of their total initial particle mass. When the $r < 2$ kpc line is younger (leftward) of the $1R_{0.5M} < r < 2R_{0.5M}$ line, we define the galaxy as being "radially inverted"; that is, the galaxy has a center that is younger than its edges, which is the opposite of the typical "inside-out" view of galaxy formation. The upper left panel of Figure 1 shows a galaxy that has been radially inverted for its entire history.

Population	Number
Full g-r Sample	1504
sSFR(1 Gyr) $> 10^{-11}$ yr^{-1}	
for $r < 2$ kpc	779
Radially Inverted at t(80%)	771
sSFR $\cap$ Radial Inversion	528

Table 2. Number of galaxies in the full g-r sample and each of its subpopulations.

The galaxies in the upper right and lower left panels are only radially inverted at late times. For the galaxy in the upper right, the different radial bins grew at roughly the same rate before radially inverting, while the galaxy in the lower left had outskirts that were notably younger than the center before inversion. The final galaxy in the lower right is never inverted. Although not shown in Figure 1, galaxies could also have been inverted at early times but appeal "normal" at late times.

Unless otherwise noted, we classify a galaxy as radially inverted by comparing when 80% of the stellar mass have been formed in each radial bin. This is consistent with the metric used by Pérez et al. (2013). They found that for 45 low mass galaxies (on average $10^{10.39}$–$10^{9.58}$ M$_\odot$), the radial gradient in the age when 80% of stellar mass has formed is quite flat, especially in the lowest mass bin (Figure 4). But there is also evidence that the lowest mass bin was distinctly radially inverted (with inner radii younger than outer) around the 50% threshold (Pérez et al. 2013, Figure 2). Unlike their sample, however, we see clear signs of radial inversion at the 80% threshold and its presence does not depend on mass for our galaxies. The prevalence of radial inversion

3.2. *Population Breakdown*

Here we look at the composition of the g-r sample and how it relates to our *D4000* sample. Figure 2 shows sSFR vs D4000 in the inner 2 kpc

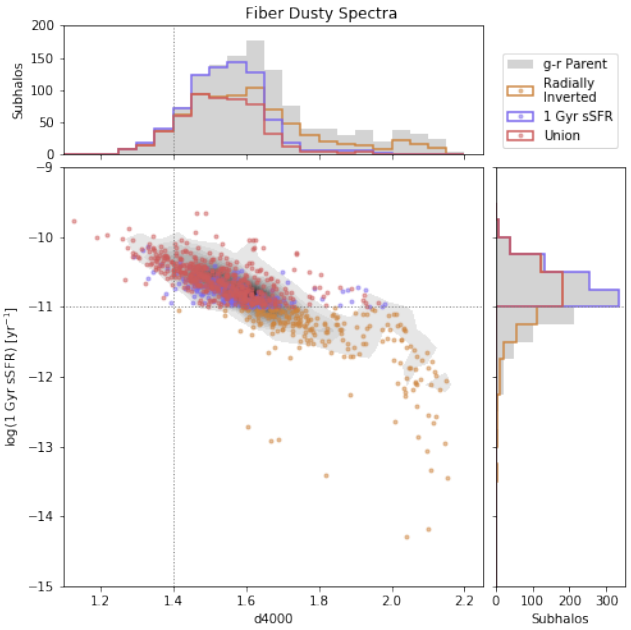

Figure 2. Average sSFR over 1 Gyr vs D4000 in the inner 2 kpc of Illustris galaxies. The sSFR was calculated directly from Illustris particles, while the D4000 was calculated from mock spectra and therefore includes dust (see Sections 2.2 and 2.3). The histograms at the top and right are not normalized. Grey contours and bars show the full g-r sample. Blue indicates galaxies that only met the sSFR $> 10^{-11}$ criterion, while orange is for those galaxies that are only radially inverted (see Section 3.1). Red dots and bars indicate galaxies that meet both criteria. The horizontal dashed line marks the sSFR $> 10^{-11}$ criterion, while the vertical line is for D4000 < 1.4. Observationally, this selection indicates sSFR $> 10^{-11}$ (Brinchmann et al. 2004). All galaxies left of the vertical line are in our final *D4000* sample.

for our g-r galaxies, where the sSFR has been averaged over the last 1 Gyr. The grey bars and contours show the g-r galaxies from which the other populations are drawn. Orange and red indicate galaxies that are "radially inverted", as defined in Section 3.1. Blue and red indicate galaxies with sSFR(1 Gyr) $> 10^{-11}$ yr^{-1}. The histograms at the top and right are not normalized, and instead show the actual count of galaxies in each bin. The horizontal and verti-

cal dashed lines are at sSFR = 10^{-11} yr^{-1} and D4000 = 1.4, respectively.

The raw numbers for each of the populations in Figure 2 are found in Table 2. Roughly 51% of the *g-r* sample is classified as radially inverted at the 80% mass level. There is also a large overlap between the sSFR and radially inverted populations (colored red in Figure 2), with roughly 68% of galaxies in each population falling in the other.

Everything left of the vertical dashed line is in our *D4000* sample of 70 galaxies. Observationally, a value of D4000 < 1.4 indicates a sSFR $> 10^{-11}$ yr^{-1} (Brinchmann et al. 2004). We see that our trends are consistent with these observations, as all 70 *D4000* galaxies have sSFR $> 10^{-11}$ yr^{-1}. All but 9, or 87%, of our *D4000* galaxies are radially inverted, which is a much higher rate than in the *parent* population with a rate of 39%.

3.3. *Central and Overall SFR*

The combination of the $g - r$ photometric selection and D4000 spectral selection is designed to return galaxies with centrally concentrated star formation. Figure 3 shows that this is indeed what is returned from Illustris. The ratio of SFR in the inner 2 kpc to the SFR of the whole galaxy is plotted against stellar mass, SFR, and sSFR. All of the (specific) star formation rates are the so-called "instantaneous" values calculated using the galaxy's gas properties. The *parent* sample is plotted as the grey contours, while the *D4000* sample is shown as green dots. The SFR is overall more centrally concentrated in the *D4000* sample, typically accounting for roughly 20% or more of the total star formation rate. From Figure 3 we can also see that the overall (s)SFR is lower for the *D4000* sample compared to the *parent*.

3.4. *Gas Content*

Characterizing the gas content of a galaxy is important for understanding both its current and potential future star formation. Figure 4 compares the total stellar mass to both the total gas mass (left) and the mass of gas for $r < 2$ kpc (right). The grey contours are for the *parent* population, while the red dots indicate the *D4000* sample. The lines are to guide the eye; they show where the gas mass is equivalent to 1%, 10%, and 100% of the stellar mass.

Overall, the *D4000* galaxies have a lower gas mass than the *parent* sample, and their total gas mass is consistently roughly 10–40% of their stellar mass. In the central region, however, the mass of gas is on par with, if not slightly higher than, the *parent* sample. This inner gas is roughly 1% of the total stellar mass for galaxies with $M_* < 10^{10.75}$ M$_\odot$, at which point the fraction steadily decreases with increasing stellar mass.

We can measure the star formation efficiency by normalizing the SFR by the mass of gas that is eligible to form stars (see Section 2.2). The inverse of this efficiency provides an estimate for how much longer the galaxy will be able to form stars at its current rate with no changes to its gas reservoir. Figure 5 shows a normalized histogram of this depletion time for both the *parent* (blue) and *D4000* (orange) samples. The histogram on the left shows the depletion time as calculated for the entire galaxy, while the times on the right are for the inner 2 kpc. Overall, galaxies in the *D4000* sample are converting gas into stars at largely the same rates at the *parent* population. In the central regions, however, we see a difference in SFE between the two populations. If the *D4000* galaxies continue at their current rate, they will convert the gas in their centers faster than the *parent* sample. They are more efficient at forming stars in their centers.

In summary, there are two important differences between the *D4000* and *parent* samples in terms of gas content. First, the gas in the *D4000* galaxies is more centrally concentrated

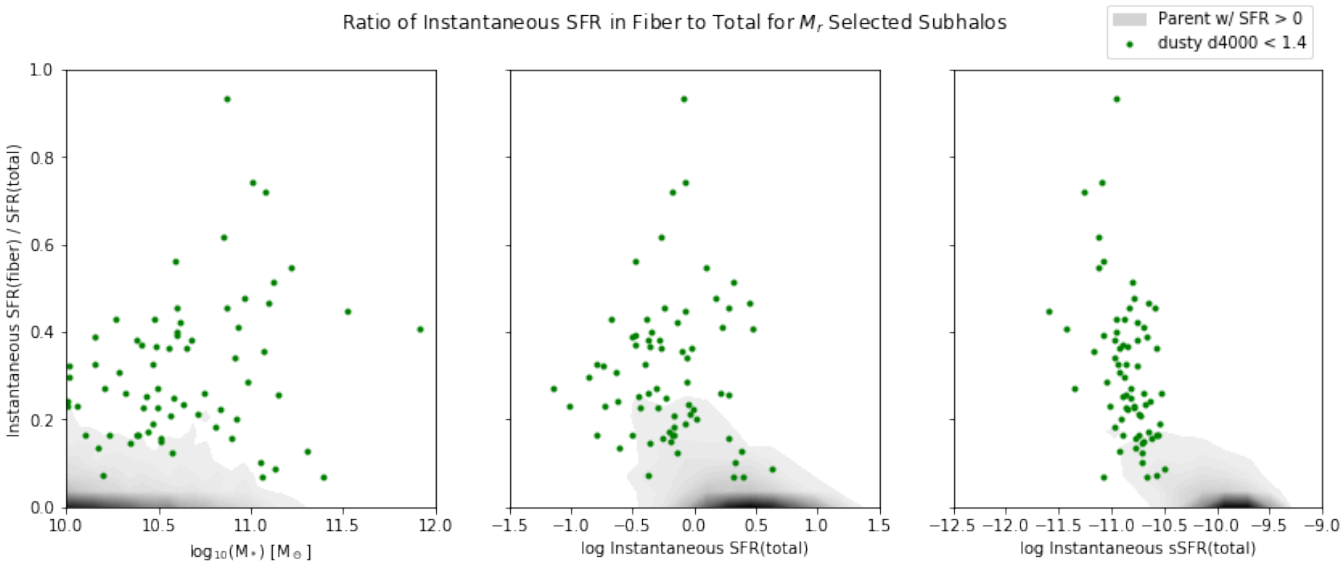

Figure 3. Ratio of instantaneous SFR in the inner 2 kpc to that in the whole galaxy, plotted against total stellar mass, whole-galaxy instantaneous SFR, and whole-galaxy instantaneous sSFR. The grey contours correspond to the *parent* sample while the green dots are the *D4000* sample. Note that not all of the parent galaxies are represented in this figure, as some have no star formation.

than in the *parent*. Second, the *D4000* galaxies are turning this centrally concentrated gas into stars more efficiently.

3.5. *Environment*

For a first look into what could explain the differences between the *D4000* galaxies and their *parent* sample, as described in the preceding subsections, we calculated the environmental density for all galaxies and separated out those galaxies which are the centers of their clusters. Of the 70 *D4000* galaxies, 19 (or 27%) of these galaxies are the central galaxy of their halo, as determined by the friends-of-friends group finder used by Illustris (Vogelsberger et al. 2014b; Nelson et al. 2015). This fraction is much lower than in the *parent* sample, where 68% of galaxies are centrals.

A measure of the environmental density for our galaxies is presented in Figure 6. Here we show the number of other galaxies with $M_* > 10^{10}$ $M_\odot$ within 2 Mpc of each *parent* (grey contours) and *D4000* (orange dots) galaxy, as a function of stellar mass. The green X's mark the 19 central galaxies. The histograms show the normalized distributions of the *parent*, *D4000*, and central *D4000* galaxies. Though there is a wide variation in densities, both populations are consistent with each other. The satellite *D4000* galaxies live in the densest environments, but are not unusual compared to the *parent* sample. The central *D4000* galaxies tend to live in lower density environments, but are still consistent with the parent.

3.6. *Merger History*

Another possible explanation for the differentiation between the *D4000* and *parent* samples is merger history. To assess the impact of merger history, we counted the number of recent noteworthy galaxy mergers experienced by both the *parent* and *D4000* sample using various criteria: mergers with stellar mass ratios greater than 1:4, 1:10, and 1:100 within both the last 1 Gyr and last 6 Gyr. Merger histories for Illustris come from Rodriguez-Gomez et al. (2015).

Figure 7 shows the number of mergers with stellar mass ratio greater than 1:4 and 1:100 for both time frames, with 1 Gyr on the left and

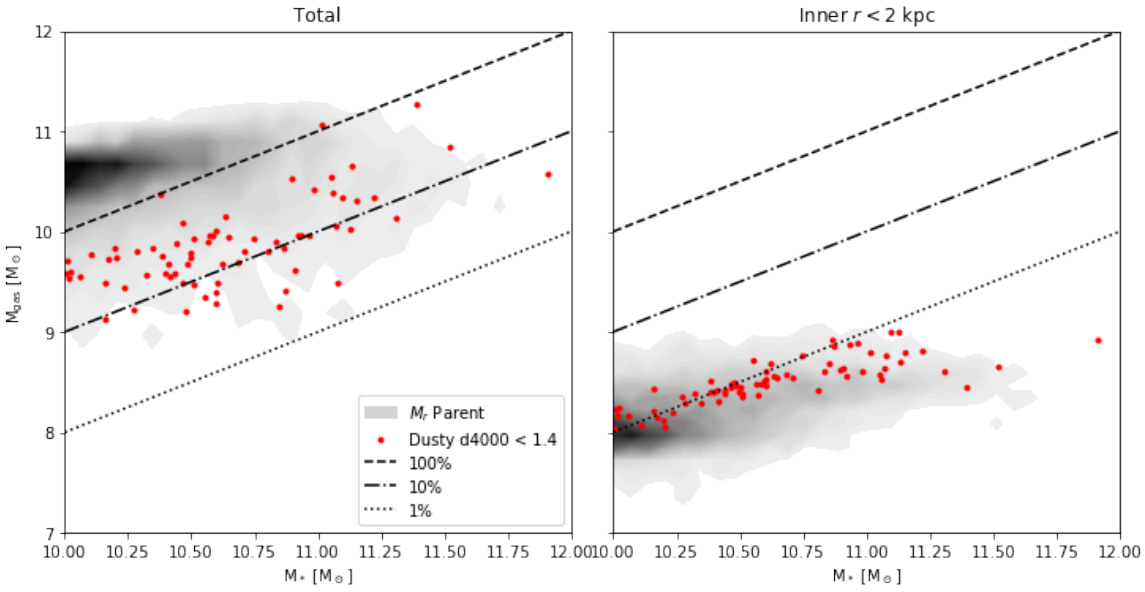

Figure 4. Gas mass, both in the whole galaxy (left panel) and in the inner 2 kpc (right panel), vs total stellar mass. The grey contours are the *parent* sample, while the red dots are the *D4000* sample. The dashed, dashed-dotted, and dotted lines are where the gas mass is 100%, 10% and 1% of the stellar mass, respectively.

6 Gyr on the right. The greyscale pixels show a 2D histogram of the *parent* sample's merger count, while the green and orange dots show the count for central and satellite *D4000* galaxies, respectively. Note that while the figure cuts off at 10 mergers, some of the *parent* galaxies experience much higher rates. Figure 7 demonstrates there is nothing unusual about the number of either major or minor mergers for the *D4000* galaxies when compared to the *parent* sample over either timescale.

4. DISCUSSION

The following discussion will use the results put forth in Section 3 to answer a series of questions in Sections 4.1–4.3.

4.1. *Did We Get What We Came For?*

We selected our *D4000* sample by applying a series of observationally-motivated photometric and spectral selection criteria to galaxies in the Illustris simulation. Specifically, the criteria were motivated by those used to obtain the MISFIReD observational sample (Tuttle & Tonnesen in prep.). It is therefore worthwhile to confirm that our selections returned simulated galaxies with the desired and observationally-expected characteristics. Figure 2 shows us that galaxies with D4000 < 1.4 in the central region also have sSFR $> 10^{-11}$ yr^{-1} in that same region, which is in agreement with observation (Brinchmann et al. 2004). Since we generated mock spectra for only the inner 2 kpc, and used a $g - r$ photometric criterion for 2 kpc $< r < 2R_{0.5M}$ to select for redder outskirts with little-to-no star formation, we expect the *D4000* galaxies to have recent, centrally concentrated star formation. Figure 3 indeed shows that these galaxies have current (specific) star formation rates that are concentrated in the central 2 kpc of the galaxies. Therefore, our selection criteria are both consistent with those used observationally, and do return galaxies with the properties we expect.

4.2. *What Is Happening in These Galaxies?*

The typical view of galaxy formation states that the centers of galaxies form first, such that they contain older stars and are subsequently

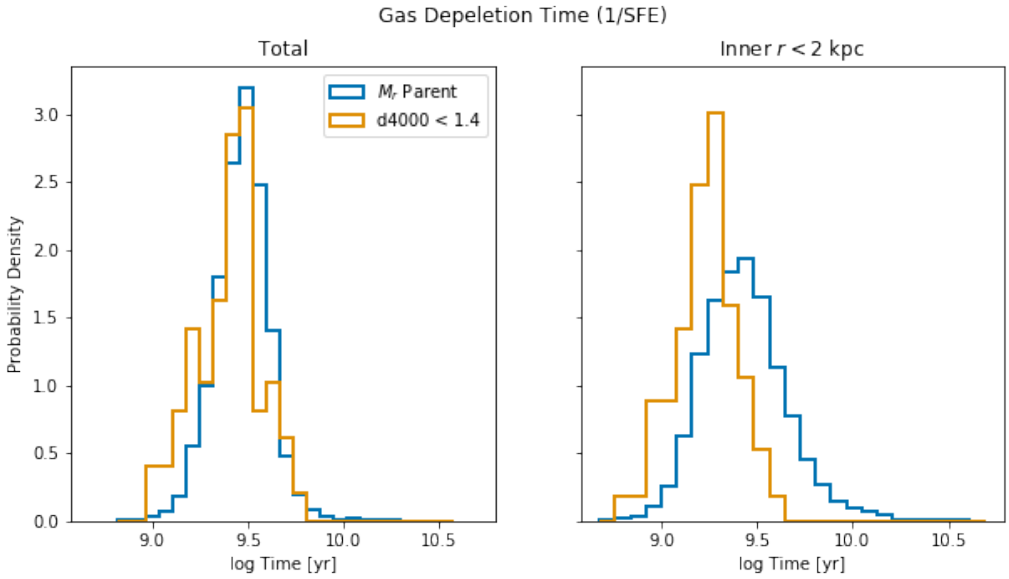

Figure 5. Gas depletion time, as estimated using the star formation efficiency (see Section 2.2). The left histogram is the time for the whole galaxy to convert its gas into stars, while the right is for the inner 2 kpc. The *parent* sample is in blue, and the *D4000* is in orange.

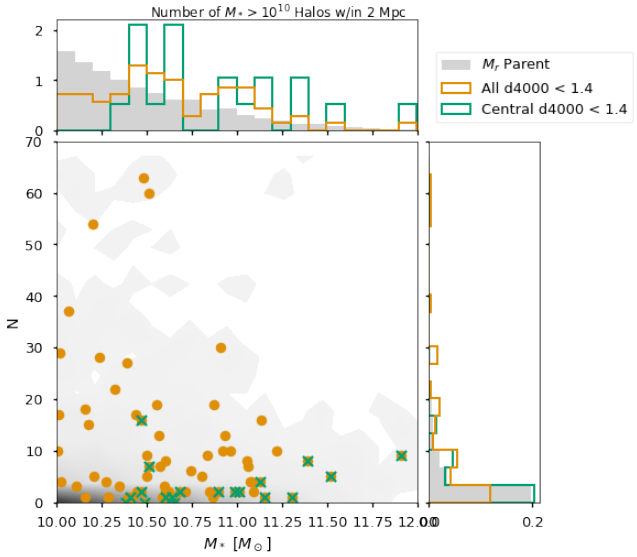

Figure 6. Number of other galaxies with $M_* > 10^{10}$ $M_\odot$ within 2 Mpc as a function of stellar mass. Histograms at the top and right are normalized. The grey contours are for the *parent* sample, while orange circles are the *D4000* galaxies. Those *D4000* galaxies that are the central galaxy of their cluster are marked with green X's.

dominated by redder light. By analyzing where the stars in our *D4000* galaxies were formed over time (in a manner consistent with observational capabilities), we see that most galaxies in our Illustris *D4000* sample have centers that are in fact younger than the outer regions. This is in addition the to recent star formation as noted in the preceding section, as the age inversion is measured from when each radial bins accrues 80% of its mass (see Section 3.2). Therefore, the *D4000* galaxies not only exhibit observational signatures that are the inverse of what's expected, but they also seem to genuinely have grown "outside-in" for at least a portion of their history.

As seen in the middle and rightmost panels of Figure 3, the *D4000* galaxies generally have lower (specific) star formation rates for the whole galaxy at the present time than the *parent* sample. Additionally, we know from the D4000 measure that these galaxies have had star formation in the past 1 Gyr. Together, we take these observations to indicate that the galaxies are in a transitional state, either ramping up or quenching their star formation. A quenching picture is favored by the lower total gas mass seen in Figure 4: a lower gas mass means the galaxies can form fewer stars in the future. If

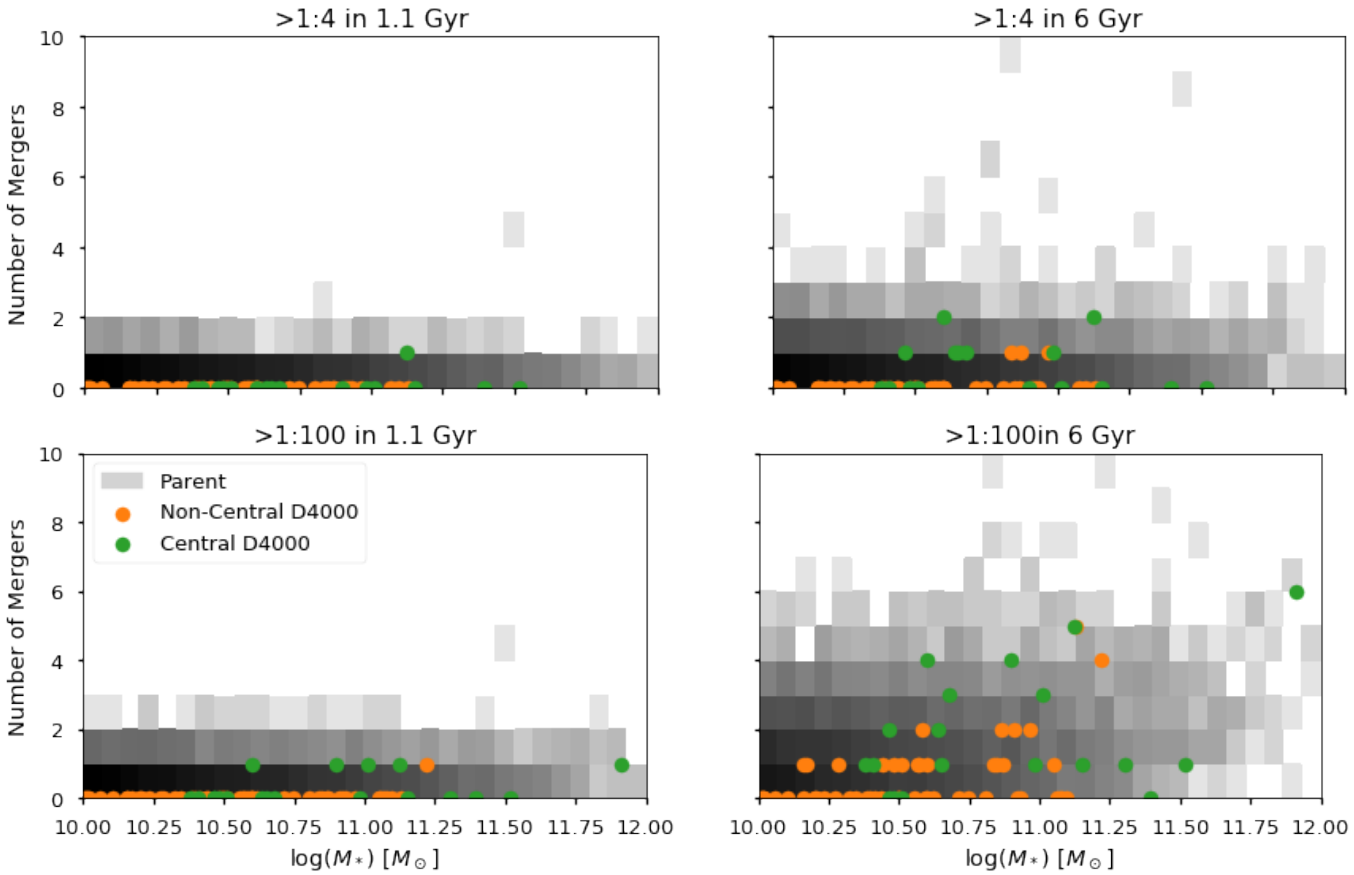

Figure 7. The number of mergers with a stellar mass ratio greater than 1:4 (top) and 1:100 (bottom) within the last 1.1 Gyr (left) and 6.0 Gyr (right), plotted against the primary galaxy's stellar mass. The grey pixels are for the *parent* sample; all plots are on the same color scale. Green dots are those *D4000* galaxies that are centrals, while the orange dots are not. Note that some galaxies in the *parent* sample have experienced many more mergers than shown.

the *D4000* galaxies are simply transitioning to being quenched, their structure would suggest that quenching as well as formation can occur from the outside-in.

Even though the *D4000* galaxies are overall gas-poor, Figure 4 also shows that within their centers, the *D4000* galaxies have roughly the same amount of gas as in the centers of the *parent* galaxies. This gas deficit at the outskirts would explain the overall lower but centrally concentrated SFR. The presence of younger centers could therefore also be explained by the inability of the outskirts to form stars. Figure 5 indicates that the central regions of the *D4000* sample are converting their gas into stars more efficiently than in the *parent*, while on the whole, both galaxy populations should (based on present conditions) keep forming stars for roughly the same amount of time. If the gas is being converted less efficiently outside of the center, perhaps because there is not much gas, then the overall rate of gas conversion could be made to appear on par with that of the *parent* sample despite the high rate in the center. A gas-deficit in the outskirts is therefore consistent with both the SFR and gas-depletion time observations presented in Section 3.

The differences between the *D4000* and *parent* samples are difficult to attribute to one particular cause, but we favor the idea that the *D4000* galaxies are undergoing quenching from the outside-in, just like they formed. In this pic-

ture, stars are still able to form at the galaxy centers, but not as much at the outskirts.

4.3. *Why Is This So?*

The *D4000* sample contains both galaxies that are the central galaxies in their clusters, and galaxies that are satellites. Though a large fraction of the *D4000* galaxies are satellites, the presence of both types indicates that the phenomenology outlined above is not restricted to either centrals or satellites. Furthermore, Figures 6 and 7 show that there are no notable differences in either environment or merger history between the *D4000* sample and its *parent* population. Therefore, at first glance, neither of these simple explanations can account for the apparent outside-in quenching. A more in-depth examination of the merger histories, beyond just the number of recent mergers, is therefore warranted.

The gas properties discussed in the preceding section could be because, at some point, gas was stripped from the outskirts. But it is worth remembering that there is also a strong connection to radial inversion, as the *D4000* sample shows a higher occurrence of this phenomena than either the *parent* or even the smaller *g-r* sample. There is no obvious reason why galaxies with younger centers should be preferentially stripped. Instead, we return to the idea of outside-in quenching that was postulated earlier: the outskirts may have quenched, thereby depleting the gas there, before the center. Yet is would remain to be see whey the galaxy centers in the *D4000* sample are more efficient at forming stars than in the *parent*.

The inadequacy of the merger histories in explaining these conclusions is especially surprising given the suggested outer stripping of these galaxies. It is possible that this phenomenology is caused by tidal stripping or from close encounters that never result in true mergers, and these kinds of encounters are not captured by a merger history. But the *D4000* galaxies do not live in environments that are much different than the *parent*, so close encounters seem unlikely. Ram pressure stripping could also remove gas, but this process would only affect central galaxies if they were very recently satellites. Determining how recently the galaxies became centrals would require further investigation. Central bars could be responsible for the denser centers but they are not well-resolved by Illustris, and there is no obvious reason why gas starvation would result in more central gas.

5. CONCLUSION

We used a series of photometric and spectral selection criteria on Illustris galaxies to look for galaxies that have red outskirts and had recent star formation in their centers. This is different from the typical picture, where galaxies have redder centers and recent star formation in the outskirts/disk. We have concluded the following about this sample:

- We found a sample of 70 galaxies that are analogous to the MISFIReD observational sample (Tuttle & Tonnesen in prep.) using our photometric and spectral selections.
- 87% of these galaxies have centers that are younger than their outskirts in addition to showing the recent star formation. This is contrary to the usual picture of galaxy evolution, in which the centers of galaxies are dominated by old stars and are believed to form first.
- The galaxies appear to be quenching from the outside-in, whereas it is usually believed that galaxies quench inside-out.
- At first glance, there is nothing significantly different about the environment or merger history for these galaxies that would explain their differences. This is something we are looking into in more detail.

Though Illustris is but one of many cosmological simulations, the MISFIReD analogues found within it suggest we interpret the observational sample as galaxies with younger centers and quenched disks; as galaxies which have evolved in a manner that is inverted from our typical picture of galaxy evolution.

The Illustris datasets contain a wealth of information that we will continue digging into. Avenues for further analysis include separating in-situ and ex-situ star formation, more in-depth analysis of the merger histories and gas and stellar evolution, including tracking our $z = 0$ *D4000* sample back in time, and trying to find a second *D4000*-like sample at $z = 0.5$ to track forward in time.

REFERENCES

Astropy Collaboration, Price-Whelan, A. M., Sipőcz, B. M., et al. 2018, AJ, 156, 123

Balogh, M. L., Morris, S. L., Yee, H. K. C., Carlberg, R. G., & Ellingson, E. 1999, The Astrophysical Journal, 527, 54

Bradley, L., Sipocz, B., Robitaille, T., et al. 2018, astropy/photutils: v0.5, , , doi:10.5281/zenodo.1340699. https://doi.org/10.5281/zenodo.1340699

Brinchmann, J., Charlot, S., White, S. D. M., et al. 2004, Monthly Notices of the Royal Astronomical Society, 351, 1151

Chabrier, G. 2003, The Publications of the Astronomical Society of the Pacific, 115, 763

Charlot, S., & Fall, S. M. 2000, The Astrophysical Journal, 539, 718

Choi, J., Dotter, A., Conroy, C., et al. 2016, The Astrophysical Journal, 823, 102

Conroy, C., & Gunn, J. E. 2010, The Astrophysical Journal, 712, 833

Conroy, C., Gunn, J. E., & White, M. 2009, The Astrophysical Journal, 699, 486

Dotter, A. 2016, The Astrophysical Journal Supplement Series, Volume 222, Issue 1, article id. 8, 11 pp. (2016)., 222, 8

Faber, S. M., Willmer, C. N. A., Wolf, C., et al. 2007, ApJ, 665, 265

Falcón-Barroso, J., Sánchez-Blázquez, P., Vazdekis, A., et al. 2011, A&A, 532, A95

Foreman-Mackey, D., Sick, J., & Johnson, B. 2014, python-fsps: Python bindings to FSPS (v0.1.1), , , doi:10.5281/zenodo.12157. https://doi.org/10.5281/zenodo.12157

Genel, S., Vogelsberger, M., Springel, V., et al. 2014, Monthly Notices of the Royal Astronomical Society, 445, 175

Nelson, D., Pillepich, A., Genel, S., et al. 2015, Astronomy and Computing, 13, 12

Paxton, B., Bildsten, L., Dotter, A., et al. 2011, The Astrophysical Journal Supplement, 192, 3

Paxton, B., Cantiello, M., Arras, P., et al. 2013, The Astrophysical Journal Supplement, 208, 4

Paxton, B., Marchant, P., Schwab, J., et al. 2015, The Astrophysical Journal Supplement Series, 220, 15

Pérez, E., Cid Fernandes, R., González Delgado, R. M., et al. 2013, The Astrophysical Journal Letters, 764, L1

Rodriguez-Gomez, V., Genel, S., Vogelsberger, M., et al. 2015, Monthly Notices of the Royal Astronomical Society, 449, 49

Salim, S., Fang, J. J., Rich, R. M., Faber, S. M., & Thilker, D. A. 2012, ApJ, 755, 105

Sánchez-Blázquez, P., Peletier, R. F., Jiménez-Vicente, J., et al. 2006, MNRAS, 371, 703

Springel, V., & Hernquist, L. 2003, MNRAS, 339, 289

Torrey, P., Snyder, G. F., Vogelsberger, M., et al. 2015, Monthly Notices of the Royal Astronomical Society, 447, 2753

Vogelsberger, M., Genel, S., Springel, V., et al. 2014a, Nature, 509, 177

—. 2014b, Monthly Notices of the Royal Astronomical Society, 444, 1518